Fractal Analysis of The Lunar Bouguer Gravity Field

Boyko Ranguelov[1], Rosen Iliev[2], Antoaneta Frantzova[3], Tzanko Tzankov

[1]Department of Applied Geophysics, University of Mining and Geology "St. Ivan Rilski", Sofia, Bulgaria

[2]Institute for Space Research and Technology, Bulgarian Academy of Sciences, Sofia, Bulgaria

[3]Climate, Atmosphere and Water Research Institute (CAWRI), Bulgarian Academy of Sciences, Sofia, Bulgaria

[4]Department of Geography and Methodology of Teaching Geography, University of Shumen „Bishop Konstantin Preslavsky, Shumen, Bulgaria

branguelov@gmail.com[1], ilievrosen@space.bas.bg[2], afrantzova@abv.bg[3], tzankov1936@abv.bg[4]

Abstract

Recent dedicated lunar gravity measure mission provided high-resolution gravity field data for the Moon. The collected data are the starting material for the construction of the latest gravity model. Like all celestial bodies, our natural satellite, is not a perfectly spherical object and its internal structure is not formed of homogeneous layers of equal thickness and gravity field varies from place to place. By measuring variations in lunar gravity can determine the density variations and deduce its internal structure. Gravitational anomalies of the Moon are caused by concentrations of huge masses of material known as "mascons". Mascons are a symbol of the periods of creation and destruction in the course of the turbulent geological history of the Moon. This article present the results of the fractal analysis of the lunar Bouguer gravity field, based on latest gravity model. The results obtained in the course of the study confirm the fractal geometry of the lunar Bouguer gravity field. The resulting fractal dimensions (D) varies from 1,4-1,5 to 2,4-2,5 and indicate a high level of gravity fragmentation. Also, the spatial relationship between Bouguer anomalies, "free-air" anomalies and the lunar digital elevation model (DEM) are considered.

Keywords: Moon, Bouguer, free-air, gravity, anomalies, fractals, GIS

Introduction

Thanks to the high achievements of scientific and technical thought in the last half century, mankind has been able to explore the space that has not been available until then. In the course of various space missions, massive data on the geology, topography and geophysics of the celestial bodies in the solar system has been gathered through space probes and powerful telescopes and satellites. There was a need to develop methods and approaches to analyze and interpret new data. In recent years, fractal analysis has become a major methodological tool for analyzing geological and geophysical processes and phenomena in others celestial bodies in the solar system [1]. Fractal Theory has been successfully applied in the analysis of Mercury's asteroid craters [2], the gravitational fields and the topography of Mars [3; 4] and Venus [3; 5], topography of the Moon [3; 6; 7; 8] and lunar gravity field [9; 1]. The results obtained in these studies give new directions for analysis and interpretation of the natural processes acting in the past and today.

The present study aims to analyze and interpret the probability of fractal structure of the Bouguer gravity anomalies within the Moon topography based on data from the latest lunar gravity model- GRGM1200A [10]. The link between Bouguer gravity anomalies (BGA) and "Free-Air" gravity anomalies (FAG) on the one hand, as well as the spatial dependencies between BGA and the lunar digital elevation model (DEM), are also discussed. The results obtained in the course of the study and the accompanying interpretations can serve as basis for further in-depth research.

Materials and Methods

Fractals analysis – methodological fundamentals

The classical example of a fractal object is defined by Mandelbrot [11]. If the length of an object P is related to the measuring unit length l by the formula:

$$P \sim l^{1-D} \qquad\qquad (1)$$

then P is a fractal and D is a parameter defined as the fractal dimension. This definition was given by B. Mandelbrot in the early 60-s of the 20-th century. His ideas support the view that many objects in nature cannot be described by simple geometric forms, and linear dimensions, but they have different levels of geometric fragmentation. It is expressed into the irregularities of the different scales (sizes) – from very small to quite big ones. This makes the measuring unit extremely important parameter, because measuring of the length, the surface or the volume of irregular geometric bodies could be obtained so that the measured size could vary hundred to thousand orders. This fact was first determined when measuring the coastal line length of West England and this gave Mandelbrot [12] the idea to define the concept of a fractal. In geology and geophysics is accepted that definition of the different "fractals" as real physical objects is most often connected to fragmentation [13]. This reveals that each measurable object has a length, surface or volume, which depends on the measuring unit and the object's form (shape) irregularity. The smaller the measuring unit is, the bigger is the total value for the linear (surface, volume) dimension of the object and vice versa. The same is valid for 2D and 3D objects.

The theoretical approach for the linear case and for the 2D and 3D cases was developed by [14; 15]. They focused the attention on the relations between the smallest measuring unit and object's size in analyzing linear (1D), 2D and 3D objects (Fig.1).
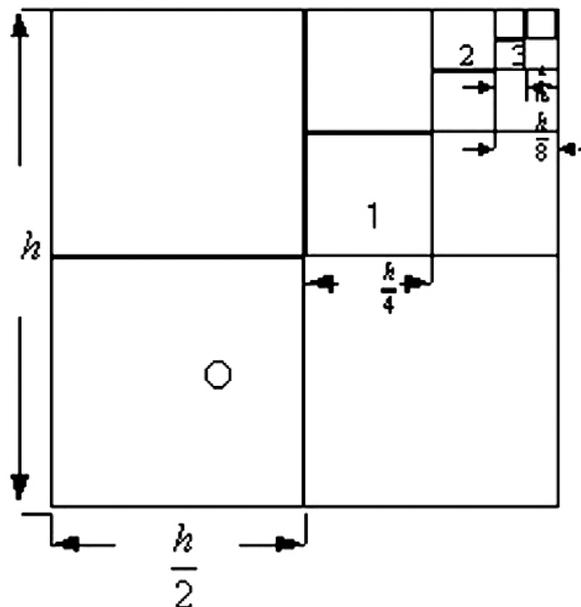

Fig.1: 2D fractal scheme – each linear element is ½ of the larger one.

If l is the measuring unit and with m we denote the obtained value for N at each measuring cycle, then the common sum of the lengths N at level m according to Turcotte [16] is:

$$N_m = (1 - p_c)\left(1 + \frac{n}{m}p_c + \left[\frac{n}{m}p_c\right]^2 \dots \left[\frac{n}{m}p_c\right]^m\right) \qquad (2)$$

where p_c denotes the probability for measuring of each length for the corresponding cycle of the measurement.

Using formulas (1) and (2) we obtain the following formulas:

$$\frac{N_{m+1}}{N_m} = 2^D \qquad (3)$$

for liner elements, and

$$\frac{N_{m+1}}{N_m} = (2^2)^D \qquad (4)$$

for any area elements (surfaces).

Another definition of a fractal dimension is related to the serial number of measurement to each of the measuring units used and the object dimensions. If the number of the concrete measurement with a selected linear unit is bigger than r, then it might be presented by:

$$N \sim r^{-D} \qquad (5)$$

and the fractal is completely determined by D as its characteristic fractal dimension.

Anti-aliasing algorithm for fractal dimension computation

In this study, the fractal dimensions of the lunar Bouguer gravity field is assumed and quantified using the anti-aliasing algorithm for calculation of raster polygons perimeter [17]. The algorithm procedure would systematically apply the moving window at every pixel, compute the surrounding pixel pattern value, and determine the associated perimeter value. Then, for each class of pixel in the raster image, a running total of perimeter values would be accumulated. Once all pixels in the raster image are processed, the running total for each pixel class is multiplied by the length of a pixel edge, resulting in the perimeters of all the polygons (areas) in the image [18]. The algorithm computed fractal dimension D using the following formula:

$$D = 2\ln P / \ln A \qquad (6)$$

Where P is the polygon's perimeter, A is its area, and ln is the natural logarithm.

Data and Software

The analysis of the lunar Bouguer gravity field was performed on the basis of GRID data (in GeoTIFF format) from the latest lunar gravity model GRGM1200A- Gravity Recovery and Interior Laboratory (GRAIL), to degree and order 1200, with sensitivity down to <5 km resolution [10]. The digital elevation model (DEM) of the lunar topography using in present study is based on data from the Lunar Orbiter Laser Altimeter (LOLA) [19], an instrument on NASA's Lunar Reconnaissance Orbiter (LRO) spacecraft [20]. Elevations are computed by subtracting the lunar reference radius of 1737.4 km [21] from the surface radius measurements.

The gravity and DEM data have been explored using Geographic Information System (GIS) - SAGA-GIS [22], QGIS [23] and Whitebox GAT 3.4 free software.

Bouguer gravity field – reflection of the lunar subsurface density variations (material pattern)

High-resolution gravity data obtained from the dual Gravity Recovery and Interior Laboratory (GRAIL) spacecraft show that the bulk density of the Moon's highlands crust is 2550 kg/m^3, substantially lower than generally assumed. When combined with remote sensing and sample data, this density implies an average crustal porosity of 12% to depths of at least a few kilometers. Lateral variations in crustal porosity correlate with the largest impact basins, whereas lateral variations in crustal density correlate with crustal composition [24]. The lunar crustal density allows construction of a global crustal thickness model according to average crustal thickness of the Moon varies between 34 and 43 km.

The Bouguer gravity anomalies represent mass anomalies within the Moon interior due to either variations in crustal thickness or variations in lunar crust or mantle density (Fig.2). Bouguer's anomalies (Δg_b) can be described using the following formula:

$$\Delta g_b = \Delta g_\varphi - 0,0419\delta H = g - \sigma_0 + 0,3086H - 0,0419\delta H \qquad (7)$$

Where δ is density and H is layer thickness.

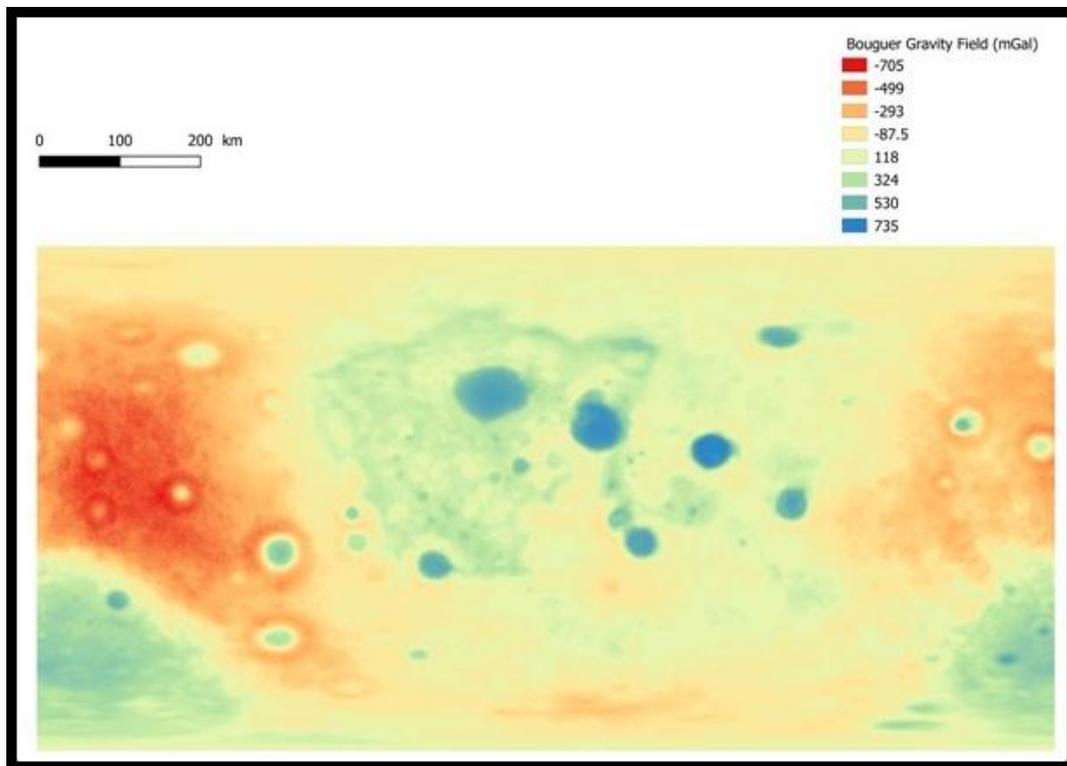

Fig.2: Spatial distribution of the lunar Bouguer gravity field

The Bouguer gravitational anomalies show a greater degree of spatial homogenity than "free-air" gravity anomalies (Fig.3). On the other hand, there is an "inverse" dependence between the spatial distribution of the Bouguer gravity anomalies and the lunar landforms (mountains and craters), which is an expected physically result (Fig.4). In practice, the lunar mountains are associated with low values of the Bouguer gravity anomalies, while the bottoms of asteroids craters are characterized by high gravity field values.
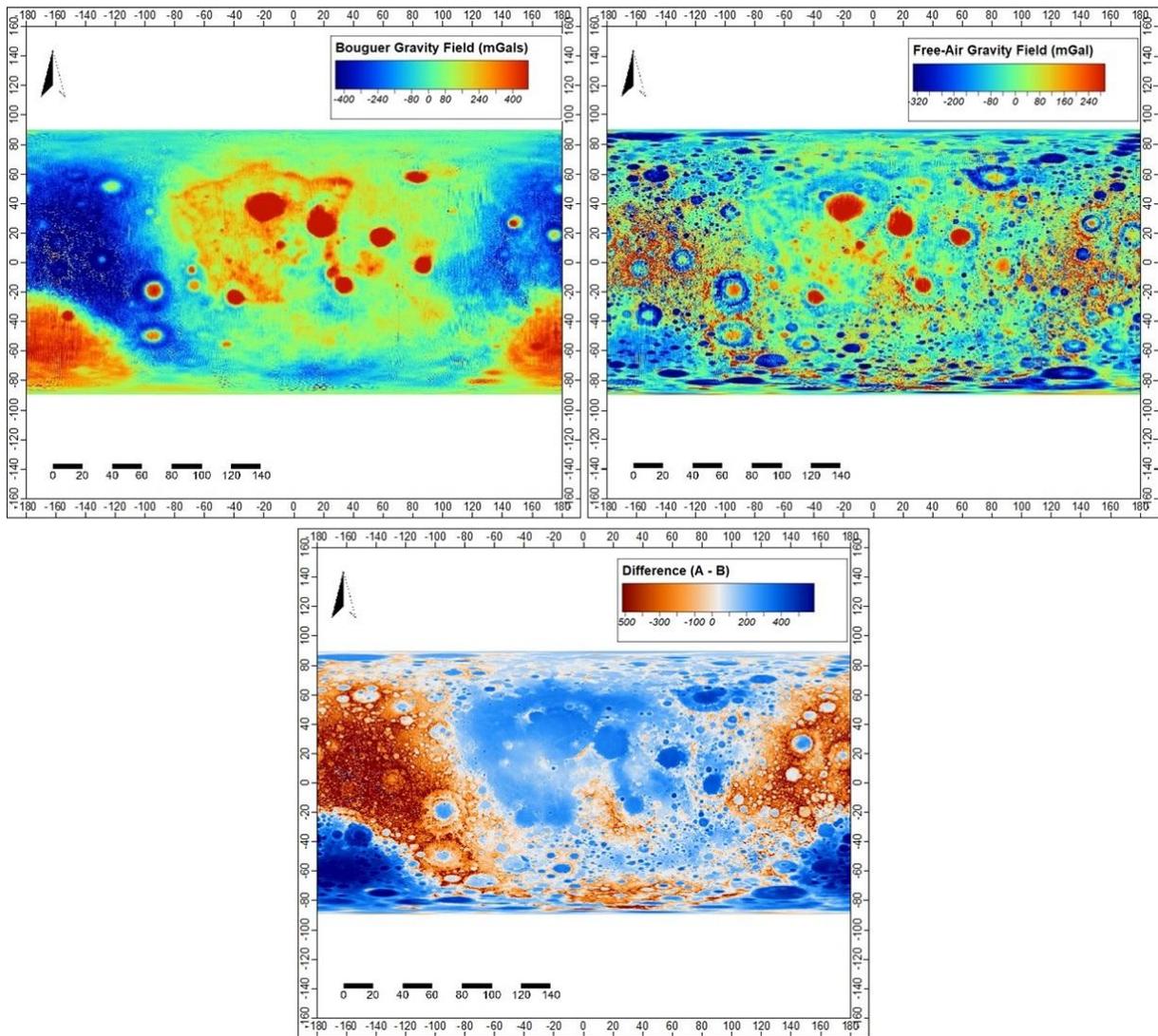
Fig.3: Comparison between lunar Free-Air and Bouguer gravity fields data using Standard Deviation (SD) approach. It is evident from the figure that there are serious differences in the absolute values of both types of gravity.
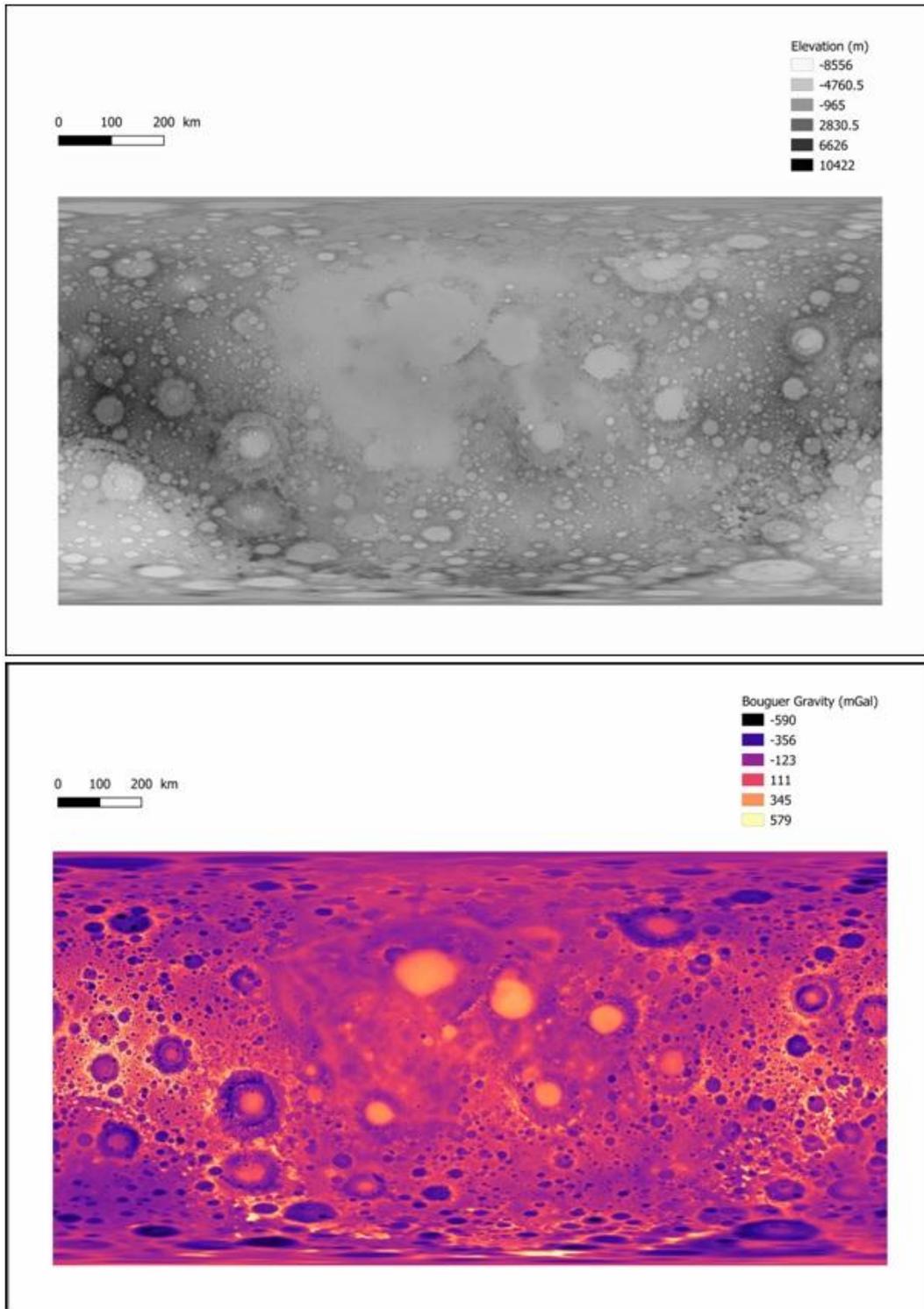
Fig.4: Spatial relation between lunar topography (above) and Bouguer gravity field (down). The areas with absolute values of the gravity field coincide spatially with the so-called "mascons".

Results and Discussion

The results of the fractal analysis of the lunar Bouguer gravity field are visual presented in Figure 5. The main conclusions and interpretations are discussed below.
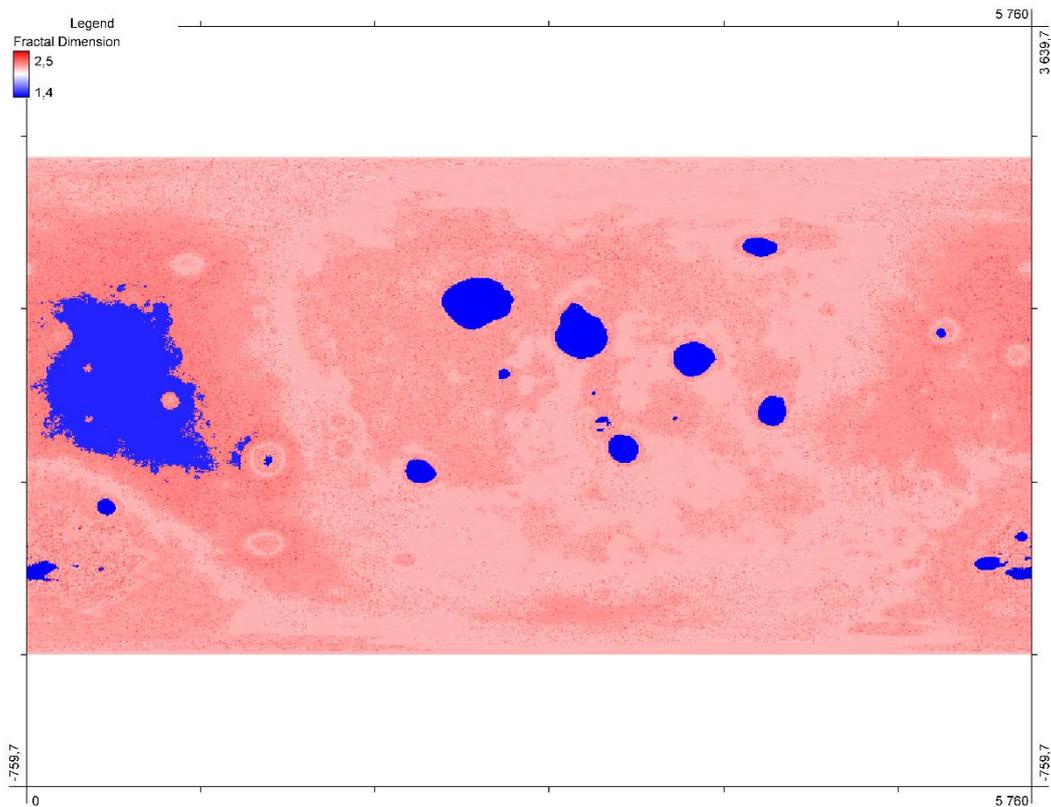

Fig.5: Fractal dimensions spatial extent of the lunar Bouguer gravity field

The results obtained in the course of the study reveal the fractal structure of the lunar Bouguer gravity field. The calculated fractal dimensions (D) ranges from 1,4-1,5 to 2,4-2,5, with the largest distribution of a dimension of 2,2-2,3 (Fig.6). Higher fractal dimension variation is an indicator of a higher degree of fragmentation of the gravity field values. This is a testimony of self-organization of geophysical fields, which is directly related to the turbulent geological history of the Moon. Periods of intense volcanic activity alternate with periods of powerful and continuous asteroid impacts.
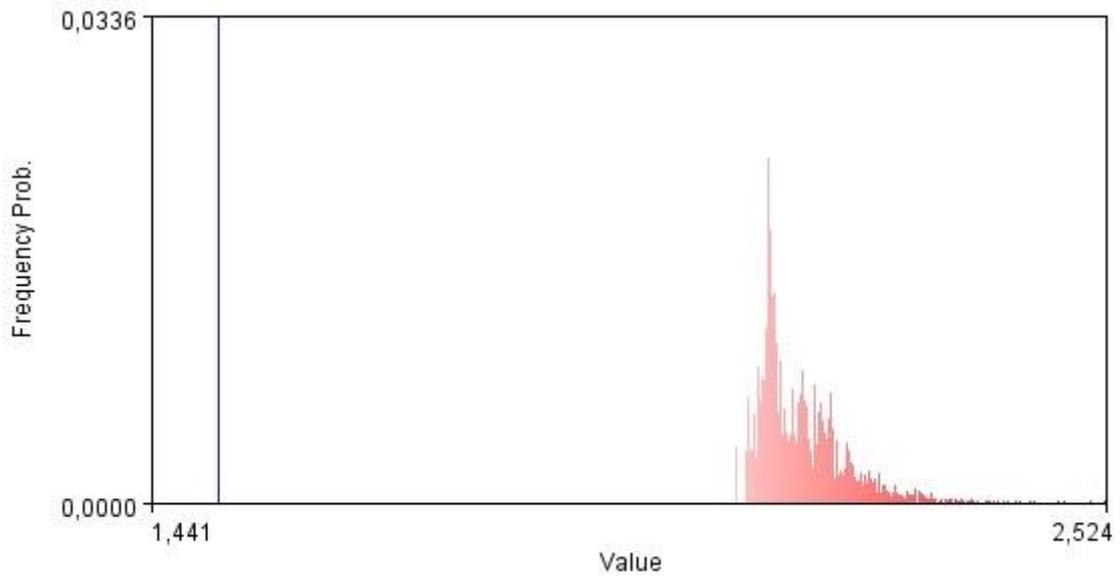
Fig.6: Fractal dimension frequency of the lunar Bouguer gravity field

The careful study of the fractal dimensions across the Moon topography (Fig.5) shows greater fractality (high values of the fractal dimension, typical for larger values of the investigated areas) mainly surrounding the areas of low fractality. This means according our interpretation that the variations of the low fractal dimensions alternate between some areas with negative Bouguer gravity anomalies (BGA) from the Moon west trough high values of BGA related to the craters of the central Moon area and decreasing to the Moon east (Fig.7). And vice-versa – the high fractal dimensions are related mostly to the central part of the high BGA, less surrounding west part of the Moon and increased values to the east.
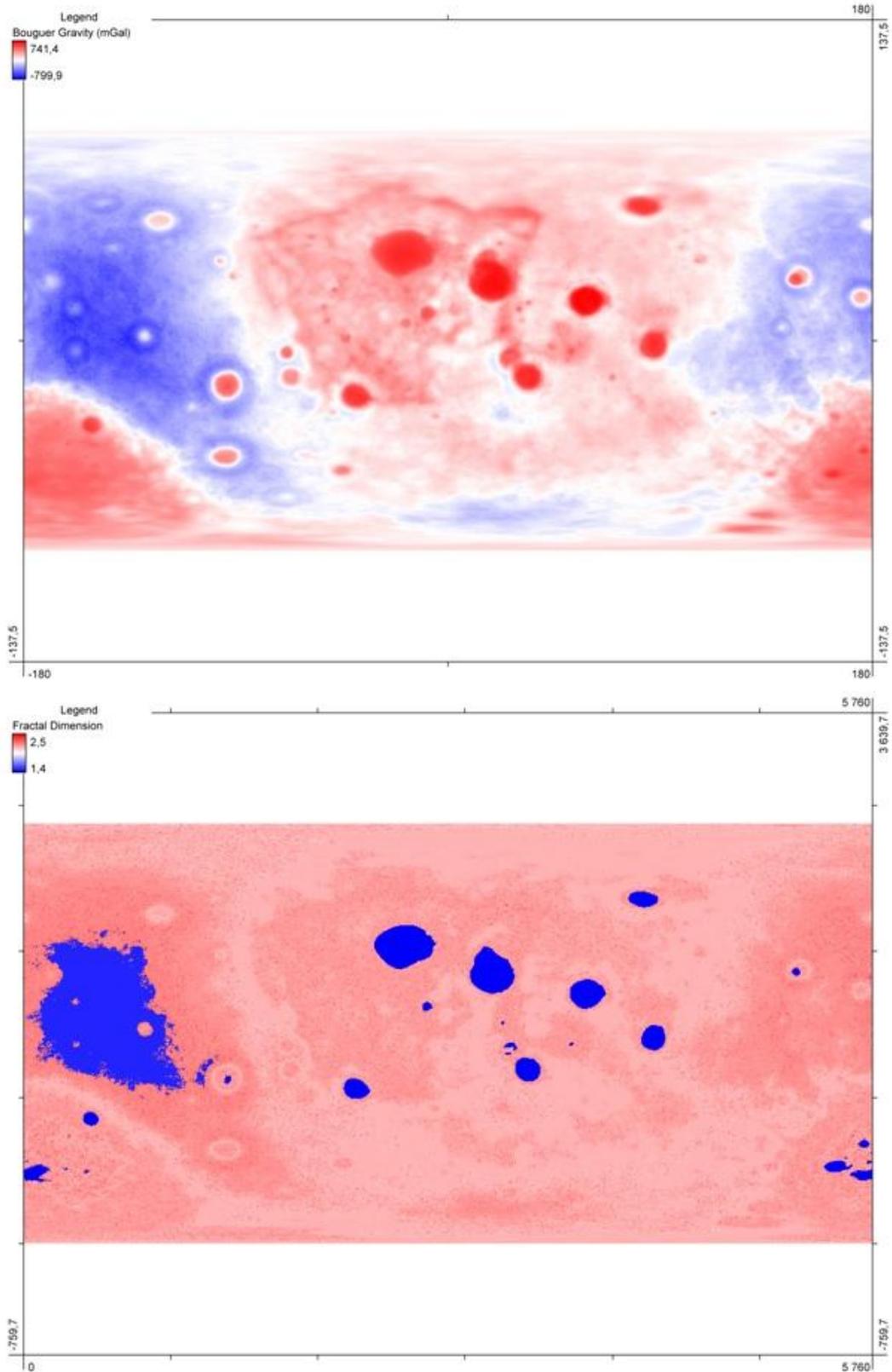
Fig.7: Spatial correlation between lunar Bouguer gravity field and its fractal dimensions. Obviously, areas with more extreme fractal dimension values are spatially matched to lunar "mascons."

Our interpretation is that BGA have predominant high values. Usually this means larger value fragmentation of the gravity – it could be related to the larger variations of the areas with higher BGA saying with other words

that the density variations cover larger areas. The low values of the fractal dimension (D) on the map speaks about larger fragmentation of the low BGA expressed in general to the low near surface density variations, as well as to the main craters of the Moon central parts shown on the selected map.

Conclusion

The comparative study of the BGA and its fractal dimensions mapping with the free-air gravity (FAG) field and lunar digital elevation model (DEM) is a next step to understanding of the Moon's interior, especially near surface gravity anomalies variations. The existence of the low fractal dimensions located over low BGA, as well as to the high level of BGA attributed to the Moon major craters is a peculiarity, which need additional investigations, comparative studies and involvement of more sophisticated data and methodologies of interpretation.

The density variations of the surface layers are completely different from these observed on the Earth's gravity field (Bouguer) anomalies. On the Earth the Bouguer anomalies are more or less related to the different geodynamics of the Earth's interior and reflect the main geotectonic structures. On the Moon – the deep distribution of the mascons is not so clear related to the fractal structure of the Bouguer gravity anomalies. The "free-air" gravity anomalies much more reflect the lunar elevation model, which is not so clearly expressed on the Earth.

The recently new discovery of the large mass under the Moon's South Pole is surprised the investigators. We consider the extended research of the relationships between BGA and FAG and the DEM of the lunar surface is necessary to reveal the peculiarities of the Earth's natural satellite.

References

[1] Ranguelov, B., Iliev, R., Tzankov, Tz., Spassov, E. (2019) Fractal analysis of the lunar free-air gravity field. To Physics Journal, Vol.2, 126-133.

[2] Mancinelli, P., Pauselli, C., Perugini, D., Lupattelli, A., Federico, C. (2014) Fractal Dimension of Geologically Constrained Crater Populations of Mercury. Pure and Applied Geophysics, Springer Verlag, Volume 172, Issue 7, 1999–2008.

[3] Turcotte, D. (1987) A fractal interpretation of topography and geoid spectra on the earth, moon, Venus, and Mars. Journal of Geophysical Research, vol. 92, 597-601.

[4] Demin, S.A., Andreev, A.O., Demina, N.Y., Nefedyev, Y.A. (2017) The fractal analysis of the gravitational field and topography of the Mars. J. Phys.: Conf. Ser. 929 012002, 1-7. Doi :10.1088/1742-6596/929/1/012002

[5] Demin, S.A., Andreev, A.O., Demina, N.Y., Nefedyev, Y.A. (2018) The fractal analysis of the topography and gravitational field of Venus. J. Phys.: Conf. Ser. 1038 012020, 1-6. Doi :10.1088/1742-6596/1038/1/012020

[6] Nefedjev, A.Y. (2003) Lunar Surface Research Using Fractal Analysis. The Journal of the Eurasian Astronomical Society, Vol. 22, Issue 4-5, 631-632. Doi.org/10.1080/10556790031000139460

[7] Baldassarri,A., Montuori,M., Prieto-Ballesteros,O., Manrubia, S.C. (2008) Fractal properties of isolines at varying altitude revealing different dominant geological processes on Earth. J. Geophys. Res., 113, E09002, doi:10.1029/2007JE003066.

[8] Huang, X, Jiang, X., Yu, T., Yin, H. (2009) Fractal-Based Lunar Terrain Surface Modeling for the Soft Landing Navigation. Second International Conference on Intelligent Computation Technology and Automation, Changsha, Hunan, China, 53-56. doi: 10.1109/ICICTA.2009.250

[9] Kumar, A.V.S., Sekhar, R.P.R., Tiwari, R.M. (2016) Fractal Analysis of lunar Gravity anomalies over the Basins of Lunar Farside. 19th National Space Science Symposium (NSSS-2016), Poster Session, Kerala, India.

[10] Goossens, S., Lemoine, F.G., Sabaka, T.J., Nicholas, J.B., Mazarico, E., Rowlands, D.D., Loomis, B.D., Chinn, D.S., Neumann, G.A., Smith, D.E., Zuber, M.T. (2016) A Global Degree and Order 1200 Model of the Lunar Gravity Field using GRAIL Mission Data. 47th Lunar and Planetary Science Conference, Houston, TX, Abstract #1484.

[11] Mandelbrot B. (1982) The Fractal Geometry of Nature. San Francisco: W.H. Freeman & Co., San Francisco, 68 p.

[12] Mandelbrot, B.B. (1967) How long is the Coast of Britannia? Statistical self-similarity and fractional dimension. Science, 156, 636-638.

[13] Korvin, G. (1992) Fractal models in the Earth Sciences. New York: Elsevier, 236 p.

[14] Turcotte, D. (1986) Fractals and Fragmentation. Journal of Geophysical Research. 91, B2, 1921-1926.

[15] Hirata T. (1989) Fractal dimension of fault system in Japan: Fractal structure in Rock geometry at various scales. Pure and Applied Geophysics, 131, 157-173.

[16] Turcotte, D. (1986) A fractal model of crustal deformation. Tectonophysics, 132, 361-369.

[17] Prashker, S. (2009) An anti-aliasing algorithm for calculating the perimeter of raster polygons. Geotec, Ottawa & Geomtics Atlantic, Wolfville, NS, CD-ROM

[18] Prashker, S. (1999) An improved algorithm for calculating the perimeter and area of raster polygons. Proceedings of the 4th International Conference on GeoComputation Mary Washington College Fredericksburg, Virginia,USA, 25 - 28 July 1999, "GeoComputation CD-ROM".

[19] Smith, D.E., Zuber, M.T., Neumann, G.A., Mazarico, E., Head, J.W., III, Torrence, M.H. and the LOLA Science Team (2011) Results from the Lunar Orbiter Laser Altimeter (LOLA): global, high-resolution topographic mapping of the Moon, Lunar Planetary Science Conference XLII, Abstract 2350.

[20] Tooley, C.R., Houghton, M.B., Saylor, R.S., Peddie, C., Everett, D.F., Baker, C.L. and Safdie, K.N. (2010) Lunar Reconnaissance Orbiter mission and spacecraft design, Space Sci. Rev., 150, 23–62, doi:10.1007/s11214-009-9624-4.

[21] Archinal, B.A. (Chair), A'Hearn, M.F., Bowell, E., Conrad, A., Consolmagno, G.J., Courtin, R., Fukushima, T., Hestroffer, D., Hilton, J.L., Krasinsky, G.A., Neumann, G.A., Oberst, J., Seidelmann, P.K., Stooke, P., Tholen, D.J., Thomas, P.C. and Williams, I.P. (2011) Report of the IAU Working Group on cartographic coordinates and rotational elements: 2009, Celestial Mechanics and Dynamical Astronomy, 109, 2, 101-135, doi 10.1007/s10569-010-9320-4.

[22] Conrad, O., Bechtel, B., Bock, M., Dietrich, H., Fischer, E., Gerlitz, L., Wehberg, J., Wichmann, V. and Boehner, J. (2015) System for Automated Geoscientific Analyses (SAGA) v. 2.1.4. Geosci. Model Dev., 8, 1991-2007, doi:10.5194/gmd-8-1991-201

[23] Thiede, R., Sutton, T., Düster, H., Sutton, M. (2014) Quantum GIS Training Manual. Locate Press, 388 p.

[24] Wieczorek, M. A., Neumann, G.A., Nimmo, F., Kiefer, W.S., Taylor, G.J., Melosh, H.J., Phillips, R.J., Solomon, S.C., Andrews-Hanna, J.C., Asmar, S.W., Konopliv, A.S., Lemoine, F.G., Smith, D.E., Watkins, M.M., Williams, J.G. and Zuber, M.T. (2013) The crust of the Moon as seen by GRAIL, Science, 339, 671-675. Doi:10.1126/science.1231530.